https://doi.org/10.5194/egusphere-2026-207
Preprint. Discussion started: 6 March 2026

Simulated temporal scaling dependencies in sub-daily precipitation

Andreas Dobler[1], Rasmus Benestad[1], Julia Lutz[1], and Kajsa M. Parding[1]
[1]The Norwegian Meteorological institute, Henrik Mohns plass 1, 0313 Oslo, Norway
Correspondence: Andreas Dobler (andreas.dobler@met.no)

Abstract. Rainfall intensity-duration-frequency (IDF) curves are an essential tool in water management, for instance in urban stormwater handling. They are commonly derived by fitting generalised extreme value distributions to observed annual maximum rainfall values, a process that requires long-term, high temporal resolution (sub-daily) observations of precipitation to ensure robust estimates. Alternatively, IDF curves can be approximated with simplified parametric mathematical expressions fitted to empirical data, providing a possibility to avoid the challenging data requirements. In this case, the parametric expression can be based on two key parameters that specify the shape of the curves: the wet-spell mean precipitation μ and the wet-spell frequency f_w. For these two parameters, robust estimates are easier to obtain.

The resulting parametric IDF curves exhibit a fractal dimension and the present study takes a step towards better understanding the conditions influencing this fractal dimension and its spatial and temporal variability. To this end, we explore the dependencies across different timescales, using hourly precipitation data from convection-permitting ($3\,\mathrm{km}$) regional climate model simulations carried out with the HCLIM model over northern Europe. The analysis is applied to HCLIM simulations driven by boundary conditions from the ERA-Interim reanalysis, as well as from the EC-Earth and GFDL-CM3 global climate models for current and future climates following the RCP8.5 scenario.

We find that the relationship between wet-spell mean precipitation for different durations, and hence the sub-daily fractal dimension, is influenced by geographical conditions, as is also the wet-spell frequency. The results are consistent across different boundary conditions representing current climate conditions (reanalysis and global climate models), and showed little sensitivity to the driving model, indicating that different meteorological phenomena prevail in different regions and that these are well represented in the models. Future climate projections show changes in the fractal dimension and wet-spell frequency ratios with a general north-south gradient. Overall, the models indicate a shift towards fewer, but more intense wet-hours per wet day.

1 Introduction

In terms of the experience and consequences, precipitation characteristics such as intensity, frequency and duration are just as vital as the total amount of precipitation and are often more apt to global warming than precipitation totals alone (Trenberth

https://doi.org/10.5194/egusphere-2026-207
Preprint. Discussion started: 6 March 2026

et al., 2003). Effective adaptation to climate change therefore requires robust and representative information on extreme events such as heavy downpour intensity lasting from minutes to hours. Intensity-duration-frequency (IDF) curves are widely used to quantify expected rainfall intensities at sub-daily timescales (Courty et al., 2019; Lutz et al., 2020; Roksvåg et al., 2021; Dyrrdal et al., 2015; Sorteberg, A et al., 2018; Koutsoyiannis et al., 1998). These curves are typically derived using extreme value theory (EVT). This requires extensive, high-quality data to reliably estimate the tails of the statistical distributions (Coles, 2001). Data paucity can thus pose a challenge when estimating return levels for rare and intense extreme rainfall on sub-daily timescales.

The use of EVT is often based on the assumption of statistical properties being stationary, whereas climate change inherently implies non-stationary behaviour. In this context, we use the term 'stationarity' in the meaning that neither statistical moments (such as the mean and standard deviation) nor probabilities change with time. An additional challenge arises from potentially inconsistent return levels across different durations, when generalised extreme value (GEV) distributions are fitted independently to annual maximum rainfall amounts for different durations. To address such inconsistencies, Roksvåg et al. (2021) suggested two post-processing methods based on quantile selection and isotonic regression.

A different approach was proposed by Vinnarasi and Dhanya (2022), using a time sliding-window framework with non-stationary modelling to study the influence of climatic variables on the distribution of precipitation extremes over Indian cities. They discovered rainfall intensities to be connected to local temperature changes, diurnal extremes changes, and global mean temperature in most locations. For Calcutta and Pune, they found additional teleconnections to the Indian Ocean Dipole and the ENSO-Modoki cycle, respectively.

There have also been efforts to derive information about IDF curves by estimating parameters that describe their shapes and characteristics (Burlando and Rosso, 1996; Koutsoyiannis et al., 1998; Yu et al., 2004; Nhat et al., 2007; Bara et al., 2009; Desramaut, 2009; Benestad et al., 2021; Parding et al., 2023), rather than estimating return levels for each duration through EVT (Rodríguez et al., 2013). Early studies of scaling and multi-scaling models for such IDF curves include Burlando and Rosso (1996), while Koutsoyiannis et al. (1998) proposed a general formula for IDF curves that is consistent with the theoretical probability foundation of block maxima. Yu et al. (2004) applied the formula $I_{\lambda d} \sim \lambda^{\beta} I_d$ for the annual maximum rainfall intensity $I_{\lambda d}$ of duration λ (in terms of the fraction of 24 hours), and found three "scaling-homogeneous regions" in terms of β over Taiwan. Nhat et al. (2007) confirmed the validity of this simple scaling rule for the Yodo River basin in Japan, and Bara et al. (2009) similarly found the scaling to be valid in Slovakia. Desramaut (2009) further demonstrated the applicability of this scaling property in Quebec, Canada, and used it for temporal downscaling of IDF curves based on global climate model output. Usually, the scaling exponent β is non-integer, i.e. the temporal scaling has a fractal dimension (Mandelbrot, 1997).

Building upon this work, Benestad et al. (2021) proposed a slightly different expression based on the two key parameters wet-day mean precipitation μ and wet-day frequency f_w to estimate return levels x_τ (in mm per duration) for different return periods τ (years) and sub-daily to daily durations L (hours):

$$x_\tau \approx \alpha\mu \left(\frac{L}{24}\right)^{\zeta} \ln(f_w \tau). \tag{1}$$

https://doi.org/10.5194/egusphere-2026-207
Preprint. Discussion started: 6 March 2026

In this equation, ζ and α are empirical scaling factors. The parameter ζ controls the shape of the IDF-curves, whereas α compensates for differences between the probability density function's upper tail of the exponential distribution and the actual empirical distribution. When ζ is non-integer, Equation 1 has a fractal dimension accounting for the fractal behaviour of precipitation scaling, consistent with earlier findings of different homogeneous scaling regions over Taiwan (Yu et al., 2004). While Caldas-Alvarez et al. (2023) already investigated the question of how scale-dependencies of thermodynamic processes influence extreme precipitation in reanalysis-driven high-resolution (3 km) climate simulations over the greater Alpine area, fractal scaling properties associated with different timescales were not explicitly addressed.

From a physical point of view, ζ is expected to reflect the relative contribution of various meteorological precipitation-generating phenomena operating at different typical timescales, like convective storms or large-scale synoptic systems. Hence, key questions are how ζ varies spatially and temporally, whether it is systematically affected by geographical factors, or whether there is a more universal quantity of $\zeta \approx 0.4$ as indicated in Benestad et al. (2021). They have shown that Equation 1 is a simplification based on the more general expression

$$x_\tau = \alpha\mu \left(\frac{L}{24}\right)^{\zeta} \ln\left[\left(f_w + \gamma \ln\left[\frac{L}{24}\right]\right)\tau\right], \tag{2}$$

which follows the same functional form as earlier scaling approaches by Yu et al. (2004), Nhat et al. (2007), Bara et al. (2009) and Desramaut (2009). While the terms μ and α here represent the daily mean precipitation intensity and the correction factor derived from daily precipitation amounts respectively (i.e., $L = 24$), analyses of sub-daily rain gauge data suggest that the wet-spell mean precipitation μ_L (in mm/duration) varies with duration L according to $\mu_L = \mu_{daily}(L/24)^{\beta+1}$. In fact, the derivation of Equation 1 in Benestad et al. (2021) was motivated by the finding of near-linear dependencies between $\ln(\mu)$ and $\ln(L)$, and between f_w and $\ln(L)$. Furthermore, with a accounting for how the correction factor α depends on timescales L following the expression $\alpha_L = \alpha_{daily}(L/24)^a$, we can write

$$\zeta = \beta + 1 + a, \tag{3}$$

where the term β accounts for the scaling relation of the wet-spell mean precipitation μ_L at different durations. Here, $\beta \in [-1, 0]$ since $\mu_L = \mu_{daily}(L/24)^{\beta+1}$ and thus $0 \leq \beta + 1 \leq 1$. For clarity, we define $\hat{\beta} = -\beta \in [0, 1]$, such that larger $\hat{\beta}$ values indicate relatively more intense short-duration precipitation than during longer-lasting events, while small $\hat{\beta}$ values correspond to more even intensities on sub-daily and daily timescales. Note that β here is related, but not equivalent to the scaling relation β (β' hereafter) used by Yu et al. (2004), Nhat et al. (2007) and Rodríguez et al. (2013).

For the wet-spell frequencies, Benestad et al. (2021) proposed $f_w(L) = f_{w,\text{daily}} + \gamma \ln(L/24)$. Hence γ describes how the frequency of events decreases with shorter durations: Large values of γ indicate that precipitation is concentrated in few hours on a wet-day, while $\gamma = 0$ would indicate precipitation on 24 hours throughout a wet-day.

This framework also provides a useful basis for assessing how IDF curves may evolve under climate change. For instance, Rodríguez et al. (2013) found that increases in the hourly precipitation intensity were proportionally (slightly) higher than those

https://doi.org/10.5194/egusphere-2026-207
Preprint. Discussion started: 6 March 2026

at daily scales, a result that would be reflected in an increase in $\hat{\beta}$. Their formulation differs slightly though, expressing return levels per hour rather than per aggregation period, implying that their key scaling parameter β' corresponds to $\zeta - 1 = \beta + a$. The interesting parameter in this context is the scaling relation, specified by the parameter β' in the expression used by Rodríguez et al. (2013) and ζ in Equation 2. We adopt Equation 2 because it explicitly incorporates the dependence of the IDF estimates on μ and f_w, whereas the earlier expressions by e.g. Rodríguez et al. (2013) are based on annual maximum intensity estimates for different time scales. This new aspect makes it possible to explore dependencies on which the IDF curves rely, even at locations with short observational records. It furthermore allows us to predict how the shape of the IDF curves change depending on changes in μ and f_w, which can be obtained from downscaled global climate model projections (Oguz et al., 2024; Benestad et al., 2025).

In summary, physical reasoning suggests that ζ is influenced by the relative intensity and γ by the relative frequency of different meteorological phenomena including both mesoscale convective systems and synoptic weather systems, such as weather fronts, mid-latitude cyclones, cut-off lows, and atmospheric rivers. Orographically forced precipitation is also expected to affect precipitation return levels associated with different timescales. A reduction in ζ (equivalently, an increase in $\hat{\beta}$) may reflect a shift toward more intense short-term convective events relative to longer-lasting cyclones (Kahraman et al., 2021), and an increase in γ would reflect that precipitation is concentrated in fewer hours. a shift towards fewer wet-hours per wet-day, i.e. fewer but more intense precipitation hours on rainy days.

2 Method

We aim to examine how the temporal scaling characteristics of IDF curves depend on location or geographical factors. However, robust estimation of the return levels underlying IDF curves requires long, high-quality sub-daily precipitation records, which are only available at a limited number of locations. To overcome this limitation, we use climate model simulations, which allow us to explore how the scaling relation varies spatially and under possible future climate conditions. Specifically, we use simulations from the regional climate model HARMONIE-Climate (Belušić et al., 2020, HCLIM hereafter) run at a convection-permitting resolution of $3\,\mathrm{km}$ over Fenno-Scandinavia. A detailed description of the model set-up can be found in Lind et al. (2020). Using kilometre-scale regional climate simulations has been shown to improve the realism of simulated weather systems compared to simulations with a coarser (e.g., $12\,\mathrm{km}$) resolution (Coppola et al., 2018). In the $3\,\mathrm{km}$ HCLIM simulations over Fenno-Scandinavia, the representation of precipitation was clearly improved by a reduction of drizzling and more intense and more frequent high-intensity events (Lind et al., 2020). Further, daily heavy precipitation frequencies, amounts and return levels are well represented (Médus et al., 2022).

Running a regional climate model at $3\,\mathrm{km}$ resolution over multi-decadal time scales remains computationally expensive. Thus, available simulations for a given domain are typically limited to one or two global climate models and emission scenarios. For the HCLIM simulations used in our analysis, lateral boundary conditions were derived from the ERA-Interim reanalysis (Dee et al., 2011) for the period 1997–2018 to simulate the recent past and serve evaluation purposes. For the current and future climate, lateral boundary conditions from the EC-EARTH (Döscher et al., 2022) and GFDL-CM3 (Donner et al., 2011) global

https://doi.org/10.5194/egusphere-2026-207
Preprint. Discussion started: 6 March 2026

climate models were used for the periods 1985–2005, 2040–2060 and 2080–2100. To reduce the resolution jump between the driving global models and the HCLIM simulations, intermediate simulations with HCLIM at 12 km resolution (HCLIM12) were employed. EC-EARTH and GFDL-CM3 were selected since they reproduce the current climate with reasonable skill and cover a spread from medium (EC-EARTH) to large (GFDL-CM3) climate-change responses under the RCP8.5 emission scenario (Lind et al., 2022). Note that the first year of each simulation period (1997, 1985, 2040, and 2080) should be treated as a spin-up year and was therefore excluded from our analysis.

To investigate how the fractal scaling parameter ζ and the concentration of precipitation in time depend on geographical factors, we analyse the underlying components. However, assessing the full effect on the IDF curves and return values is challenging since we do not have sufficiently long series to estimate the return levels x_τ and the correction factor exponent a for long return periods. Thus, we focus on the parameters $\hat{\beta}$ and γ, assuming that the 20-year simulation periods are sufficient for estimating wet-day mean precipitation and wet-day frequency. Spatial variations and changes in $\hat{\beta}$ and γ then provide a guiding framework for differences in the scaling relation ζ and γ of the IDF estimation following Equation 2

3 Results

As an initial step of our analysis, we have used Equation 1 as a conceptual 'toy model' and explored a range of scenarios to assess how variations in f_w, μ and ζ affect the resulting return level curves (Figure 1). The purpose of this sensitivity experiment was to identify which modifications have the strongest effect on the outcome. In this particular example, the mean precipitation intensity μ has a direct proportional effect and, thus, the largest influence on the return levels. Variations in the wet-day frequency f_w have a more moderate effect, while changes in the fractal scaling ζ affect the shape of the curves. This simple IDF framework relies on the assumption that $|f_w| \gg |\gamma \ln \left[\frac{L}{24}\right]|$ in Equation 2, which is more accurate for longer sub-daily durations ($L >$ 9hrs) than shorter ones. For instance Benestad et al. (2021) give $\gamma \approx 0.06$ and $f_w \geqslant 0.3$.

Figure 2 shows the spatial distributions of hourly and daily wet-spell intensities μ and wet-spell frequencies f_w derived from the high-resolution HCLIM evaluation simulations driven by ERA-Interim boundary conditions. Both are influenced by geographical conditions, with the highest estimates for $\mu(L = 1hr, 1day)$ near the coasts, while the lowest values occur in mountainous regions and the inland. Wet-spell frequencies are highest along the coast and in high elevation regions. Hourly intensities generally exceed the corresponding daily values, indicating that precipitation tends to occur in short, intense bursts rather than being evenly distributed over a full day. Similarly, daily wet-spell frequencies $f_{w,\mathrm{daily}}$ are higher than $f_{w,\mathrm{hourly}}$, implying that precipitation events on a wet-day on average last less than 24 hours.

Geographical patterns of the estimated scaling parameters $\hat{\beta}$ and γ from the HCLIM evaluation simulations are shown in Figure 3. Consistent with the findings for μ and f_w, the temporal scaling of precipitation intensity is influenced by geographical factors. $\hat{\beta}$ ranges from 0.1 to 0.4, with lower values (≈ 0.1) in high-elevation regions and higher values over the North Sea (≈ 0.4). The latter may be associated with regions of frequent frontal and cyclonic activity, where storm-track density is high. In contrast, lower $\hat{\beta}$ values in mountainous areas may reflect the typical presence of orographic precipitation as opposed to frontal or cyclonic precipitation.

https://doi.org/10.5194/egusphere-2026-207
Preprint. Discussion started: 6 March 2026

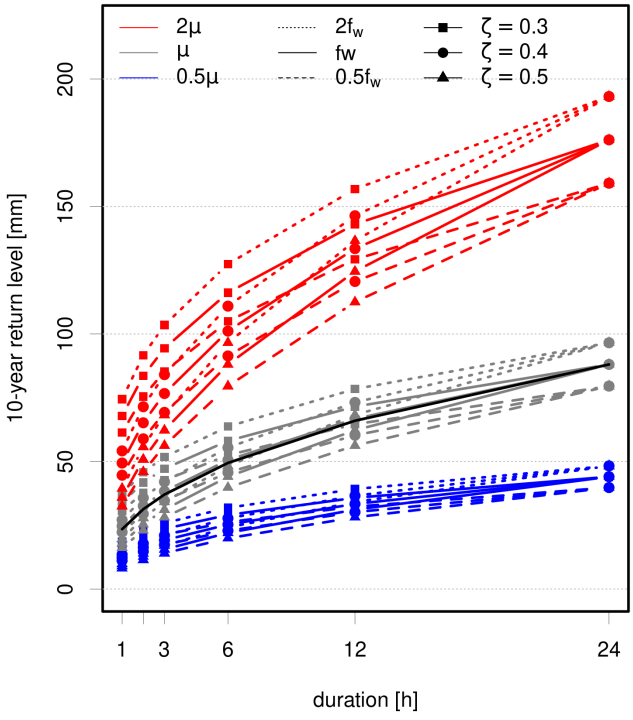

Figure 1. Results for 10-year return levels (in mm) for different durations (hours on the x-axis) from the 'toy model' with combinations of different input parameters. The black solid line marks the original curve based on station data from Bjørnholt (Oslo). Red, gray and blue lines are created using 2, 1 and 0.5 times the original μ value of 8.7 mm/day. Dotted, solid and dashed lines are from 2, 1, and 0.5 times f_w from Bjørnholt (0.36) respectively. The squares, circles and triangles denote curves generated with ζ values of 0.3, 0.4 and 0.5 (original value: $\zeta = 0.416$).

The HCLIM simulations likewise suggest that geographical factors influence how wet-spell frequency depends on duration, but the spatial patterns differ from those of μ_L (Figure 3). Here, γ can be interpreted as an indicator of how the frequency of events decreases with sub-daily timescales, since $f_w(L) = f_{w,\text{daily}} + \gamma \ln(L/24)$ and $\ln(L/24) < 0$ for $L < 24$. According to the model results, $\gamma \in [0.02, 0.09]$. The highest values for γ can be found off the west coast of Norway, in a region strongly affected by low-pressure systems. Here, wet-day frequencies are highest (Fig. 2) and the decrease towards shorter duration frequencies is largest. Thus γ is large and hourly frequencies are much lower than daily ones (Fig. 2), which can be related to relatively fast-moving (frontal) precipitation systems interspersed with dry hours. Farther inland, particularly in the mountainous regions, γ is smaller, indicating more persistent precipitation systems. Here, also the difference between hourly and daily wet-spell frequencies f_w is smaller (Fig. 2).

Similar geographical patterns appear when HCLIM is driven by boundary conditions from the EC-EARTH and GFDL-CM3 global climate models for the current climate (Figs. S1 and S2), indicating that these patterns are robust and largely independent of the forcing boundary conditions. Furthermore, a linear regression analysis across all three boundary-condition data sets (Fig.

https://doi.org/10.5194/egusphere-2026-207
Preprint. Discussion started: 6 March 2026

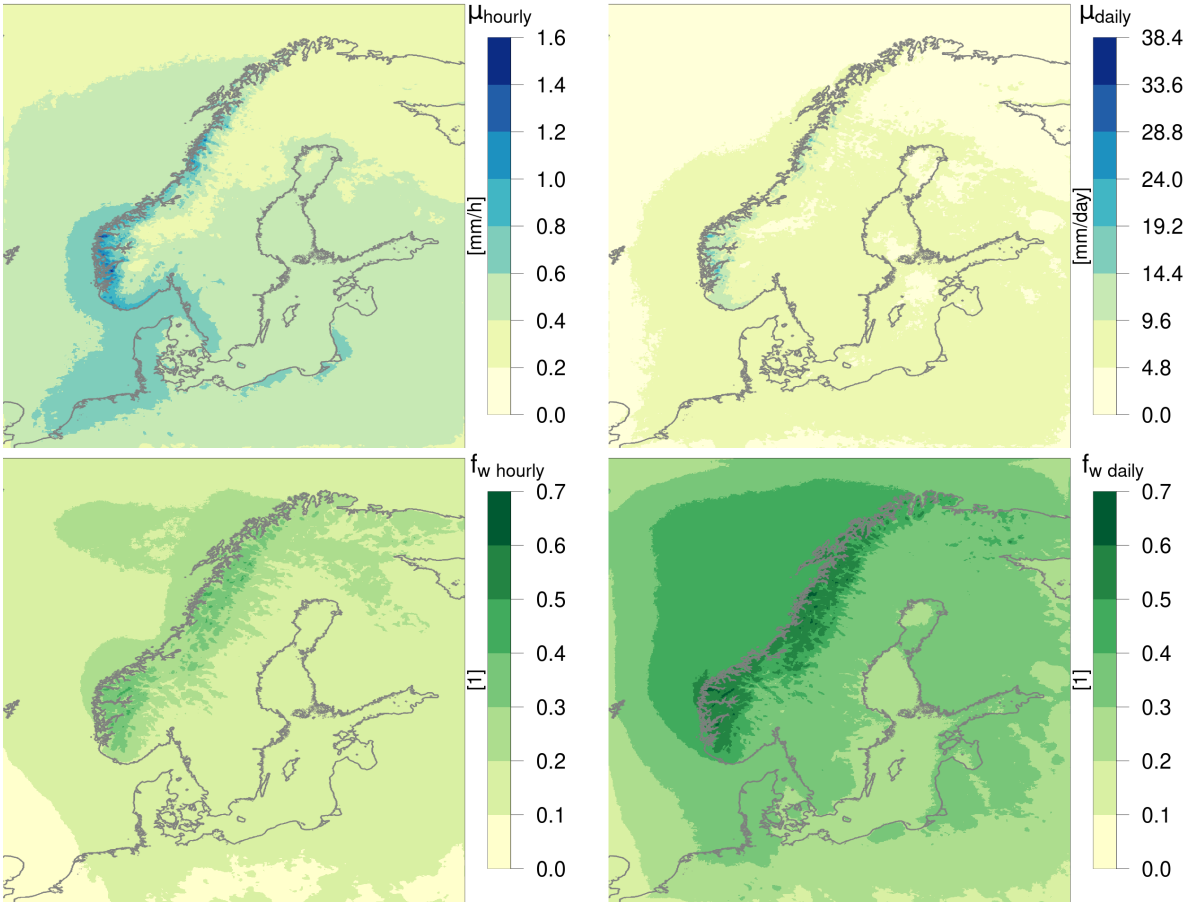

Figure 2. Estimates of hourly (left) and daily (right) wet-spell intensities (top) and wet-spell frequencies (bottom) based on the ERA-Interim driven HCLIM evaluation simulations for the period 1998–2018.

S3) shows that $\ln(u_L)$ is close to being proportional to $\hat{\beta}\ln(L/24)$ and that γ scales linearly with $\ln(L)$. This provides further support of the findings in Benestad et al. (2021).

3.1 Future changes

The HCLIM simulations were further analysed to assess how the parameters $\hat{\beta}$ and γ may change with global warming. Figure 4 shows the simulated differences in the two parameters between the present period (1985–2005) and the far future period 2081–2100, based on HCLIM simulations driven by the EC-EARTH and GFDL-CM3 global climate models following the RCP8.5 scenario. The results suggest that $\hat{\beta}$ may increase by a factor as large as 1.6 in northern Fennoscandia, while showing a slight decrease along the southern Norwegian west coast. Although the spatial patterns are generally similar in the two simulations, the more warming GFDL-CM3-driven run exhibits more pronounced changes over several regions, particularly across large

https://doi.org/10.5194/egusphere-2026-207
Preprint. Discussion started: 6 March 2026

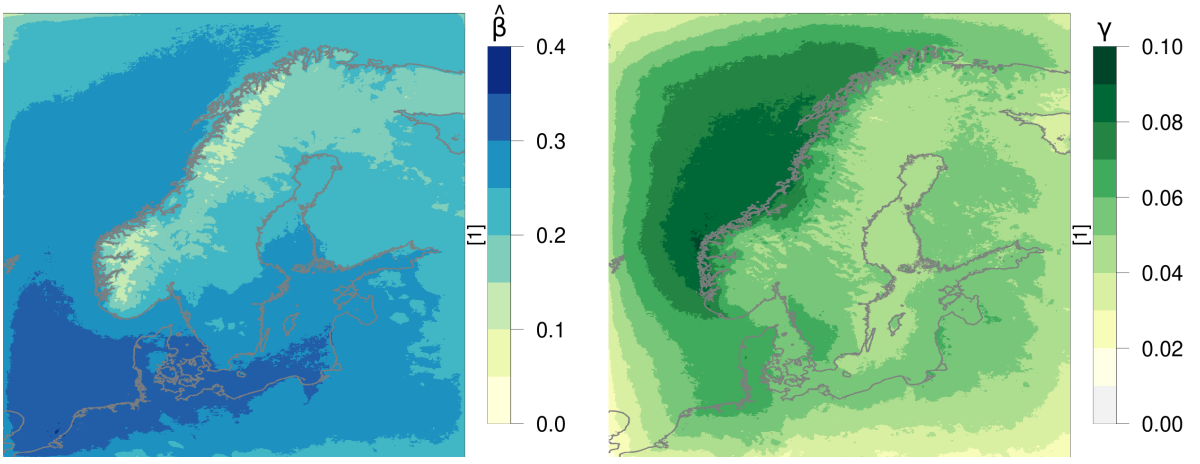

Figure 3. Estimates of the $\hat{\beta}$ (left) and γ (right) parameter based on the ERA-Interim driven HCLIM evaluation simulations for the period 1998–2018 and the equations $\mu(L) = \mu_{daily}(L/24)^{1-\hat{\beta}}$ and $f_w(L) = f_{w,\text{daily}} + \gamma \ln(L/24)$.

parts of Sweden. Corresponding results for γ indicate a similar north-south contrast, with increases in the northern parts of the domain and decreases in the southern, especially south-western, regions.

Due to the pronounced presence of stochastic decadal variability (Deser et al., 2012, 2020), it is difficult to say whether these changes represent statistically robust long-term trends connected to global warming. Conventional significance testing is of limited value in this case, as it does not account for chaotic decadal variability. However, the change signals for the far-future period closely resemble those in the near-future period (2041–2060; Fig. S4-S6), albeit with more pronounced amplitudes. Also the similar but stronger change patterns in the GFDL-CM3-driven simulation indicates that at least part of the simulated changes is related to global warming.

Fig. 5 shows the projected changes in daily and hourly wet-spell mean precipitation μ. In most regions, intensities increase more for hourly than for daily durations, except in areas such as the south-western Norwegian coast, where $\hat{\beta}$ decreases (Fig. 4). This supports our interpretation of $\hat{\beta}$ as a parameter linking precipitation scaling to the wet-spell mean precipitation μ: increases in $\hat{\beta}$ correspond to relatively larger increases in μ at shorter durations compared to longer ones.

Projected changes in daily and hourly wet-spell frequencies are presented in Figure 6. Note that especially hourly frequencies decrease over large parts of the domain. Exceptions can be found extending from the southern to the central Norwegian west-coast and towards the north-western corner of the domain. For daily frequencies, the GFDL-CM3-driven simulation features a pronounced area of increase. In the northern half of the domain the daily wet-spell frequencies tend to decrease less, or increase more, than the hourly wet-spell frequencies, independent of the general sign in the frequency changes. This is consistent with the simulated increases in γ (Fig. 4).

As an example on how changes in $\hat{\beta}$ and γ reflect local intensity and frequency changes, different duration changes for four locations in Norway (see Fig. 4) are shown in Fig. 7. Increases in $\hat{\beta}$ clearly correspond to a larger increase for the shorter duration intensities (all locations except Bergen), and increases in γ (all except Oslo in the HCLIM EC-EARTH simulation)

https://doi.org/10.5194/egusphere-2026-207
Preprint. Discussion started: 6 March 2026

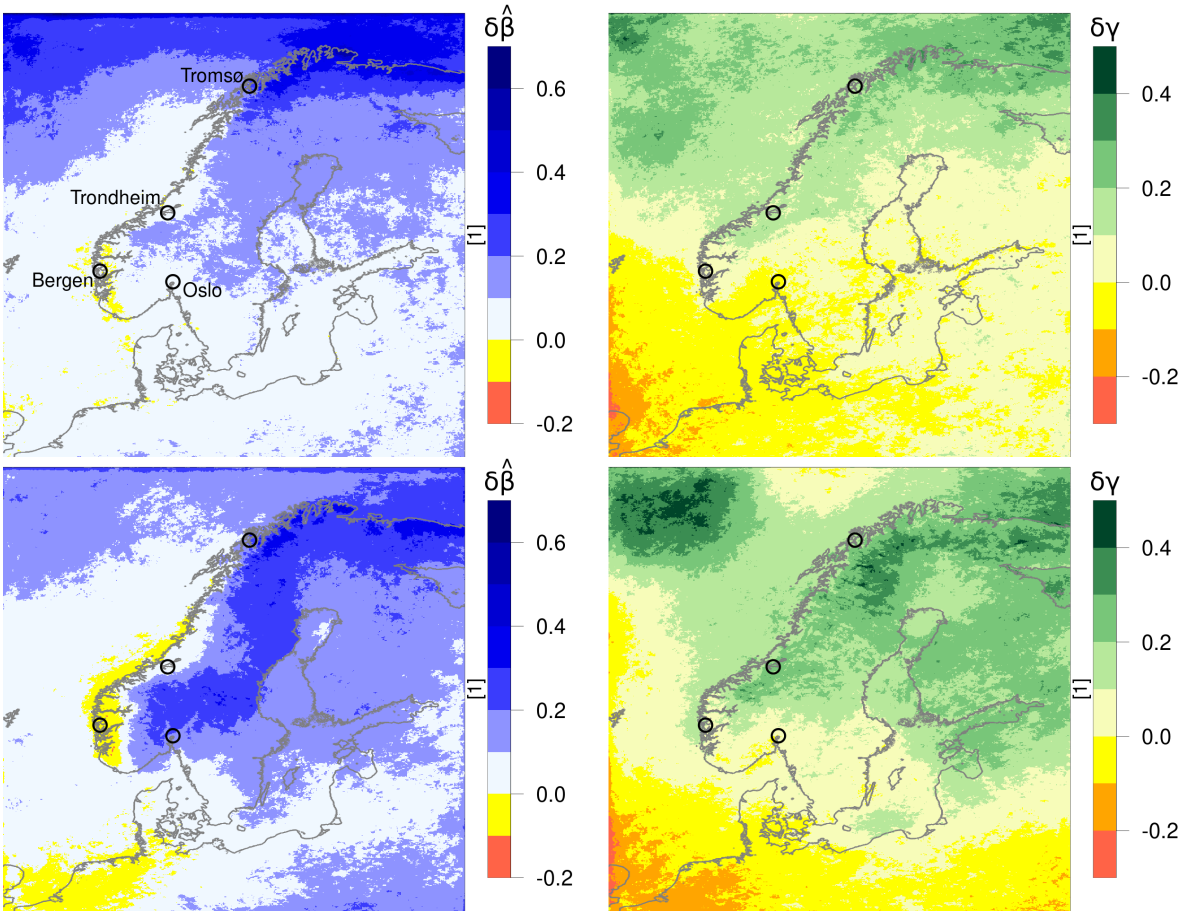

Figure 4. Relative changes in $\hat{\beta}$ (left) and γ (right) for the EC-EARTH (top) and GFDL-CM3 (bottom) driven HCLIM simulation for the far future period 2081-2100 following RCP8.5 compared do the current climate. The circles show four example locations.

denote a relative decrease in the shorter duration frequencies. For instance for Tromsø, the daily frequency of precipitation increases, while the hourly decreases. For the estimates of the return levels and IDF curves based on Equation 2, changes in $\hat{\beta}$ and γ may act in opposing directions for sub-daily durations: While μ increases more at short durations (increase in $\hat{\beta}$), yielding larger increases in short duration return levels, smaller increases or decreases in f_w at short durations (increase in γ) result in smaller return level increases.

4 Discussion

Although we did not directly assess how the fractal properties of ζ depend on geographical conditions, partial insight was obtained by examining estimates for $\hat{\beta}$. Previous studies (Benestad et al., 2012a, b, 2019) suggested that the divergence between sub-daily rainfall statistics and the tails of the exponential distribution is constant in space (i.e., that a is a constant). However,

https://doi.org/10.5194/egusphere-2026-207
Preprint. Discussion started: 6 March 2026

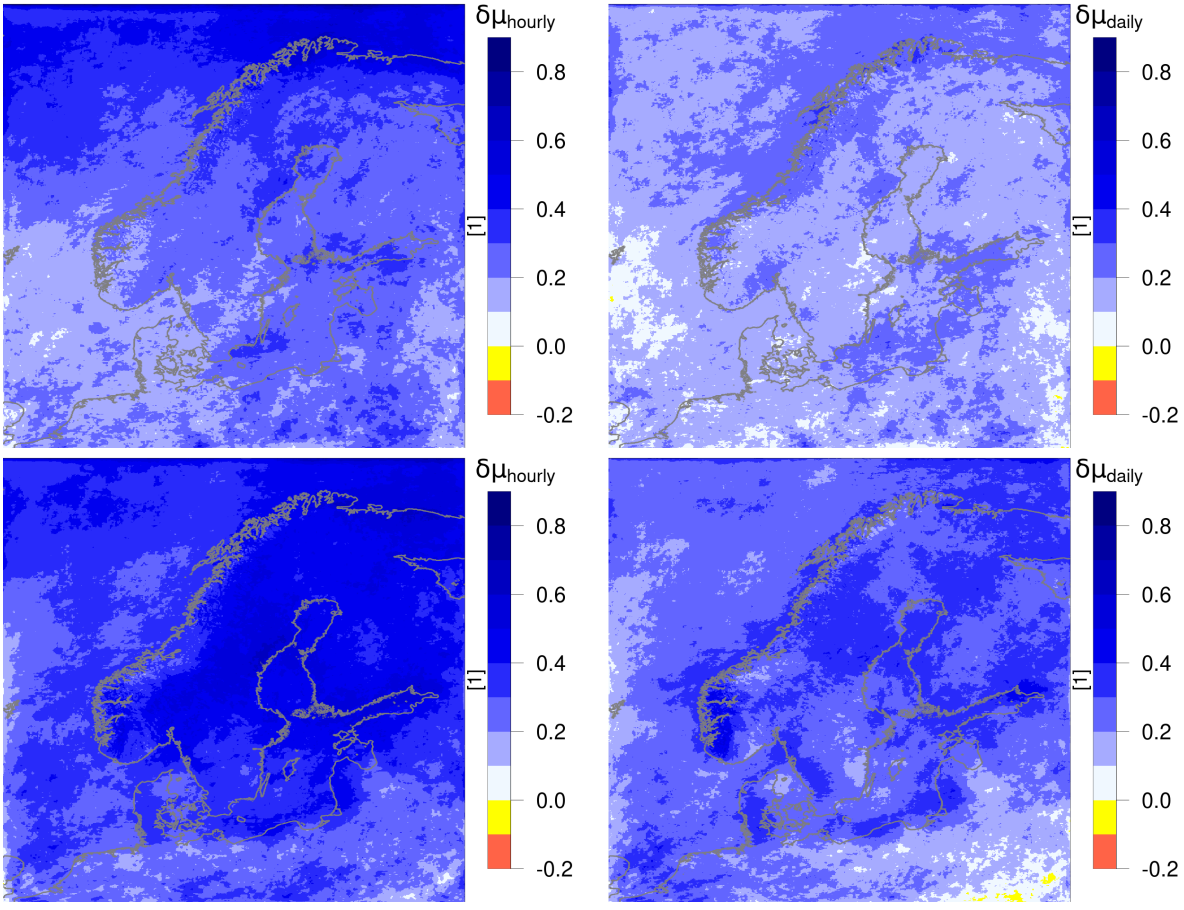

Figure 5. Relative changes in hourly (left) and daily (right) mean wet-spell intensity for the EC-EARTH driven (top) and GFDL-CM3 driven HCLIM simulation for the far future period 2081-2100 following RCP8.5 compared to the current climate.

since we limited our analysis to β, and not the full IDF curves, we did not test this assumption. Additionally, the spatial variability of γ provides information on how geographical factors affect the frequency of sub-daily rainfall.

We assume that simulations from the HCLIM model capture the essential atmospheric phenomena and processes, but acknowledge that model deficiencies and systematic biases may result in misrepresentations of precipitation statistics. Nevertheless, the model results seem plausible and show only weak sensitivity to the choice of boundary conditions when reproducing current climate conditions.

An analysis of simulated precipitation for the future was used to estimate the implications of changes in β ($\hat{\beta}$) and γ on the IDF curves based on Equation 2. The resulting future outlooks depend on the choice of the driving global climate model, which is not surprising, as even a single climate model can produce different long-term climate evolutions from small perturbations in initial conditions (Deser et al., 2012, 2020). Hence, these results should only be interpreted as a projection of a possible future climate and mostly serve as illustrative examples of changes in β and γ in space and time and the usage of our proposed

https://doi.org/10.5194/egusphere-2026-207
Preprint. Discussion started: 6 March 2026

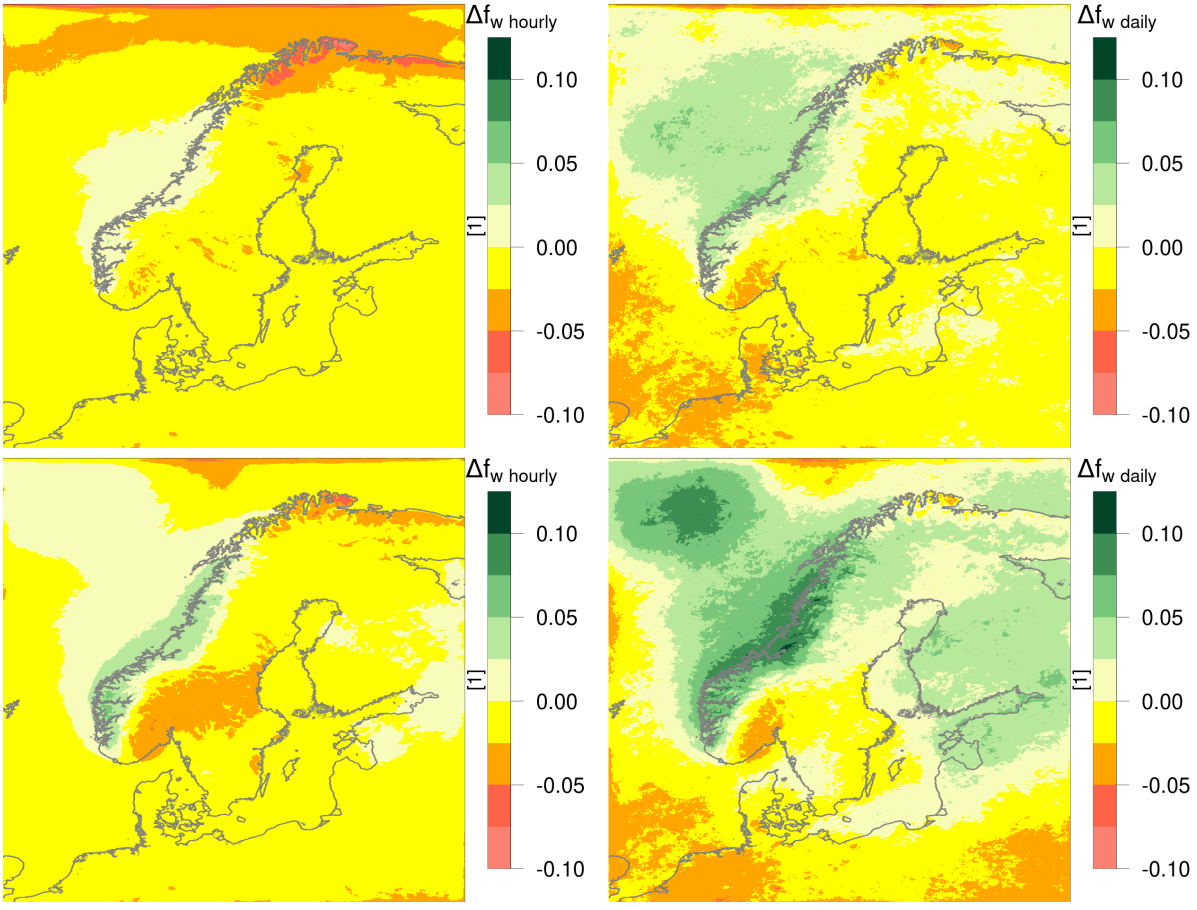

Figure 6. Absolute changes in hourly (left) and daily (right) wet-spell frequency for the EC-EARTH driven (top) and GFDL-CM3 driven HCLIM simulation for the far future period 2081-2100 following RCP8.5 compared to the current climate.

scaling framework for sub-daily to daily wet-spell frequencies and intensity relations. However, the projected patterns seem to scale with increasing warming, indicating at least some relation between climate warming and the precipitation statistics.

Our results suggest that the magnitude of IDF curves is more strongly affected by the wet-day mean precipitation μ than by the wet-day frequency f_w. The sub-daily scaling factor ζ and the frequency parameter γ are likely influenced by geographical factors. This interpretation is consistent with the observation that IDF curves differ from region to region (Parding et al., 2023). The parameters are changing under continued global warming. A plausible explanation is that precipitation-generating processes operating on different timescales respond differently to climate change. An alternative approach to test this would be to explicitly identify different types of precipitation events in the data and analyse how their relative number evolves over time. However, such an analysis lies outside the scope of the present study. Finally, the picture may change slightly with different seasons, as summer precipitation is more strongly influenced by convective systems, whereas autumn and winter precipitation is more often associated with large-scale cyclonic systems.

https://doi.org/10.5194/egusphere-2026-207
Preprint. Discussion started: 6 March 2026

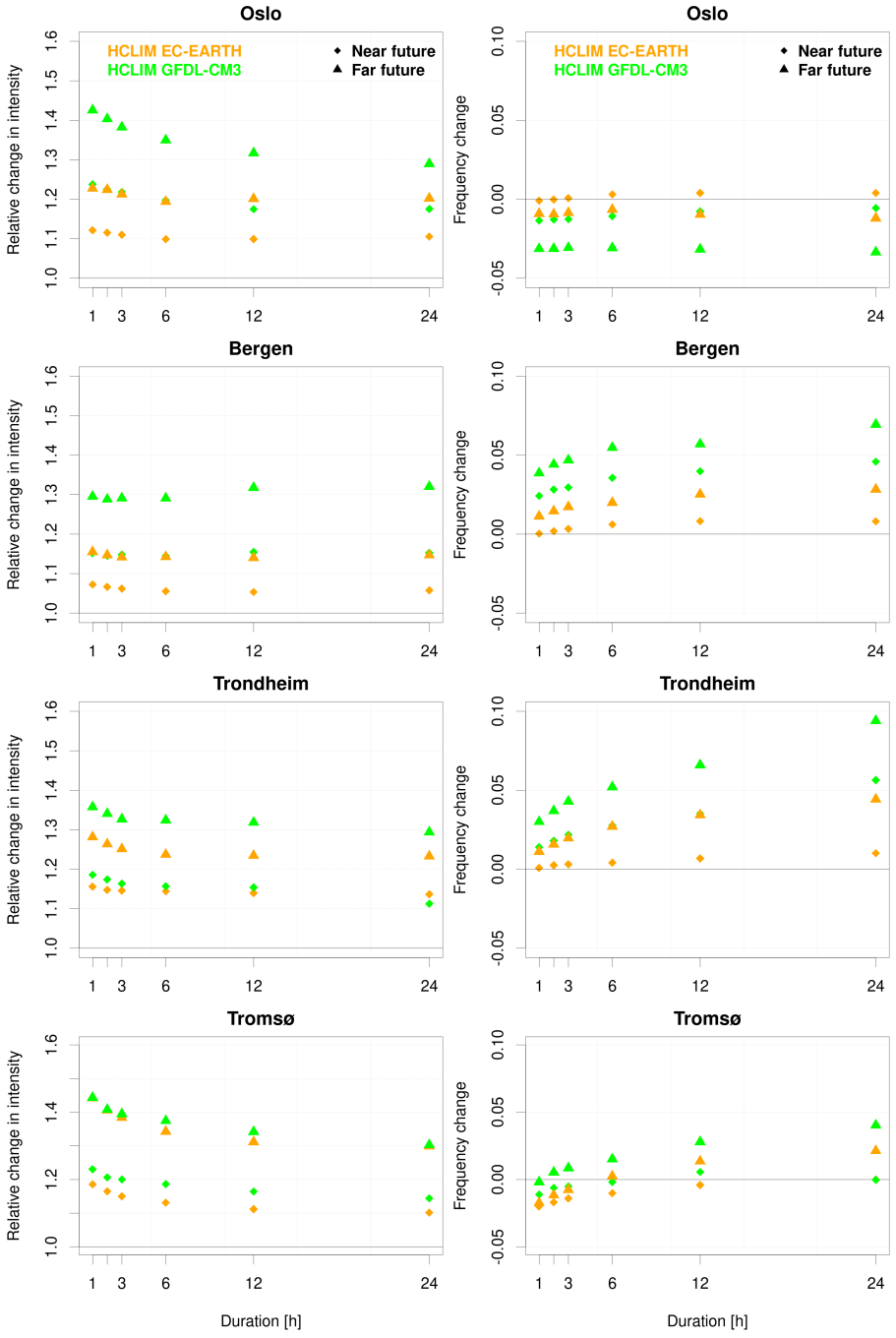

Figure 7. Relative change in mean wet-spell intensity (left) and absolute changes in frequency (right) for the HCLIM grid-points closest to Oslo, Bergen, Trondheim and Tromsø.

https://doi.org/10.5194/egusphere-2026-207
Preprint. Discussion started: 6 March 2026

5 Conclusions

We demonstrate that insight on how the fractal scaling of sub-daily rainfall may be affected by local conditions can be gained using high-resolution convective-permitting climate model simulations. The results suggest that the fractal dimension characterising the dependencies across temporal scales vary in space, possibly reflecting the influence of different precipitation-generating meteorological phenomena. Future climate projections indicate that the relationship between precipitation at different time scales may change in a warmer climate, implying that frequencies and intensities of convection, cyclones, frontal systems, cut-off lows, and orographic precipitation may respond differently to global warming.

We propose a framework summarizing the scaling of sub-daily to daily wet-spell frequencies and intensities in two single parameters ($\hat{\beta}$ and γ) making it possible to provide single maps of their geographic dependencies and changes. Our results show an increase in wet-spell intensities with a general intensification towards shorter durations (increase in $\hat{\beta}$). For frequencies, we find mostly a shift towards fewer wet-hours per wet-day (increase in γ). Overall this indicates a shift towards fewer but more intense precipitation hours on rainy days which is in agreement with findings of Guilloteau et al. (2025) over western North America.

This study also demonstrates the values of high-resolution regional climate model simulations for testing hypotheses in contexts where consistent, dense, and temporally high-resolved long-term observational networks are lacking. The use of convective-permitting regional climate model simulations to assess methods associated with empirical-statistical downscaling (ESD), such as the fractal scaling of IDF curves, illustrates how dynamical downscaling and ESD can be combined. Facilitating such cross-connecting efforts is a key objective within the EURO-CORDEX programme (Jacob et al., 2020).

Code and data availability. An *R* markdown script for the 'toy model' used to conduct the return-level sensitivity test is available at https://doi.org/10.6084/m9.figshare.31057399. The simple IDF equation (Eq. 1) is part of the R-package 'esd' that is freely available at https://github.com/metno/esd.

The convection-permitting NorCP HCLIM data from the EC-Earth RCP8.5 driven simulation covering the time periods 1986–2005, 2041–2060 and 2081–2100 used in this study are available at https://doi.org/10.11582/2025.v5h1qkwp. The corresponding data from the GFDL-CM3 RCP8.5 driven simulation is available at https://doi.org/10.11582/2025.laixk5j6 and the ERA-Interim driven simulation (1998–2018) at https://doi.org/10.11582/2025.00064. *R* data files with derived statistics (μ, f_w, β, γ) from the different HCLIM runs are available at https://doi.org/10.6084/m9.figshare.31057471.

Author contributions. AD did the modelling and the analysis of the results; REB was involved in conceptualising the paper, writing it up and developed the toy model used for Figure 1; KMP and JL contributed to writing the paper.

Competing interests. None

https://doi.org/10.5194/egusphere-2026-207
Preprint. Discussion started: 6 March 2026

Acknowledgements. We thank the World Climate Research Program Coupled Modeling Working Group, responsible for the Coupled Model Intercomparison Project (CMIP), and the climate modelling groups developing, maintaining and running the HCLIM, EC-EARTH, and GFDL models. We also want to acknowledge the ECMWF and its development and publication of the ERAINT reanalysis. This work uses HCLIM regional climate model data from the NorCP project, which is a Nordic collaboration involving climate modelling groups from the Danish Meteorological Institute (DMI), Finnish Meteorological Institute (FMI), Norwegian Meteorological Institute (MET Norway) and the Swedish Meteorological and Hydrological Institute (SMHI). This work was also motivated by discussions within EURO-CORDEX regarding the value of combining ESD and dynamical downscaling.

https://doi.org/10.5194/egusphere-2026-207
Preprint. Discussion started: 6 March 2026

References

Bara, M., Kohnová, S., Gaál, L., Szolgay, J., and Hlavčová, K.: Estimation of IDF curves of extreme rainfall by simple scaling in Slovakia, Contributions to Geophysics and Geodesy, 39, 187–206, 2009.

Belušić, D., de Vries, H., Dobler, A., Landgren, O., Lind, P., Lindstedt, D., Pedersen, R. A., Sánchez-Perrino, J. C., Toivonen, E., van Ulft, B., Wang, F., Andrae, U., Batrak, Y., Kjellström, E., Lenderink, G., Nikulin, G., Pietikäinen, J.-P., Rodríguez-Camino, E., Samuelsson, P., van Meijgaard, E., and Wu, M.: HCLIM38: a flexible regional climate model applicable for different climate zones from coarse to convection-permitting scales, Geoscientific Model Development, 13, 1311–1333, https://doi.org/10.5194/gmd-13-1311-2020, 2020.

Benestad, R. E., Nychka, D., and Mearns, L. O.: Spatially and temporally consistent prediction of heavy precipitation from mean values, Nature Climate Change, 2, 544–547, https://doi.org/10.1038/nclimate1497, 2012a.

Benestad, R. E., Nychka, D., and Mearns, L. O.: Specification of wet-day daily rainfall quantiles from the mean value, Tellus A: Dynamic Meteorology and Oceanography, 64, 14 981, https://doi.org/10.3402/tellusa.v64i0.14981, 2012b.

Benestad, R. E., Parding, K. M., Erlandsen, H. B., and Mezghani, A.: A simple equation to study changes in rainfall statistics, Environmental Research Letters, 14, 084 017, https://doi.org/10.1088/1748-9326/ab2bb2, 2019.

Benestad, R. E., Lutz, J., Dyrrdal, A. V., Haugen, J. E., Parding, K. M., and Dobler, A.: Testing a simple formula for calculating approximate intensity-duration-frequency curves, Environmental Research Letters, 16, 044 009, https://doi.org/10.1088/1748-9326/abd4ab, 2021.

Benestad, R. E., Parding, K. M., and Dobler, A.: Downscaling the probability of heavy rainfall over the Nordic countries, Hydrology and Earth System Sciences, 29, 45–65, https://doi.org/10.5194/hess-29-45-2025, 2025.

Burlando, P. and Rosso, R.: Scaling and muitiscaling models of depth-duration-frequency curves for storm precipitation, Journal of Hydrology, 187, 45–64, https://doi.org/10.1016/s0022-1694(96)03086-7, 1996.

Caldas-Alvarez, A., Feldmann, H., Lucio-Eceiza, E., and Pinto, J. G.: Convection-parameterized and convection-permitting modelling of heavy precipitation in decadal simulations of the greater Alpine region with COSMO-CLM, Weather and Climate Dynamics, 4, 543–565, https://doi.org/10.5194/wcd-4-543-2023, 2023.

Coles, S. G.: An Introduction to Statistical Modeling of Extreme Values, Springer, London, 2001.

Coppola, E., Sobolowski, S., Pichelli, E., Raffaele, F., Ahrens, B., Anders, I., Ban, N., Bastin, S., Belda, M., Belusic, D., Caldas-Alvarez, A., Cardoso, R. M., Davolio, S., Dobler, A., Fernandez, J., Fita, L., Fumiere, Q., Giorgi, F., Goergen, K., Güttler, I., Halenka, T., Heinzeller, D., Hodnebrog, Ø., Jacob, D., Kartsios, S., Katragkou, E., Kendon, E., Khodayar, S., Kunstmann, H., Knist, S., Lavín-Gullón, A., Lind, P., Lorenz, T., Maraun, D., Marelle, L., van Meijgaard, E., Milovac, J., Myhre, G., Panitz, H.-J., Piazza, M., Raffa, M., Raub, T., Rockel, B., Schär, C., Sieck, K., Soares, P. M. M., Somot, S., Srnec, L., Stocchi, P., Tölle, M. H., Truhetz, H., Vautard, R., de Vries, H., and Warrach-Sagi, K.: A first-of-its-kind multi-model convection permitting ensemble for investigating convective phenomena over Europe and the Mediterranean, Climate Dynamics, 55, 3–34, https://doi.org/10.1007/s00382-018-4521-8, 2018.

Courty, L. G., Wilby, R. L., Hillier, J. K., and Slater, L. J.: Intensity-duration-frequency curves at the global scale, Environmental Research Letters, 14, 084 045, https://doi.org/10.1088/1748-9326/ab370a, 2019.

Dee, D. P., Uppala, S. M., Simmons, A. J., Berrisford, P., Poli, P., Kobayashi, S., Andrae, U., Balmaseda, M. A., Balsamo, G., Bauer, P., Bechtold, P., Beljaars, A. C. M., van de Berg, L., Bidlot, J., Bormann, N., Delsol, C., Dragani, R., Fuentes, M., Geer, A. J., Haimberger, L., Healy, S. B., Hersbach, H., Hólm, E. V., Isaksen, L., Kållberg, P., Köhler, M., Matricardi, M., McNally, A. P., Monge-Sanz, B. M., Morcrette, J., Park, B., Peubey, C., de Rosnay, P., Tavolato, C., Thépaut, J., and Vitart, F.: The ERA-Interim reanalysis:

https://doi.org/10.5194/egusphere-2026-207
Preprint. Discussion started: 6 March 2026

configuration and performance of the data assimilation system, Quarterly Journal of the Royal Meteorological Society, 137, 553–597, https://doi.org/10.1002/qj.828, 2011.

Deser, C., Knutti, R., Solomon, S., and Phillips, A. S.: Communication of the role of natural variability in future North American climate, Nature Climate Change, 2, 775–779, https://doi.org/10.1038/nclimate1562, 2012.

Deser, C., Lehner, F., Rodgers, K. B., Ault, T., Delworth, T. L., DiNezio, P. N., Fiore, A., Frankignoul, C., Fyfe, J. C., Horton, D. E., Kay, J. E., Knutti, R., Lovenduski, N. S., Marotzke, J., McKinnon, K. A., Minobe, S., Randerson, J., Screen, J. A., Simpson, I. R., and Ting, M.: Insights from Earth system model initial-condition large ensembles and future prospects, Nature Climate Change, 10, 277–286, https://doi.org/10.1038/s41558-020-0731-2, 2020.

Desramaut, N.: Estimation of intensity duration frequency curves for current and future climate, M.S. tesis, McGill, Canada, https://escholarship.mcgill.ca/concern/theses/mg74qn568, 2009.

Donner, L. J., Wyman, B. L., Hemler, R. S., Horowitz, L. W., Ming, Y., Zhao, M., Golaz, J.-C., Ginoux, P., Lin, S.-J., Schwarzkopf, M. D., Austin, J., Alaka, G., Cooke, W. F., Delworth, T. L., Freidenreich, S. M., Gordon, C. T., Griffies, S. M., Held, I. M., Hurlin, W. J., Klein, S. A., Knutson, T. R., Langenhorst, A. R., Lee, H.-C., Lin, Y., Magi, B. I., Malyshev, S. L., Milly, P. C. D., Naik, V., Nath, M. J., Pincus, R., Ploshay, J. J., Ramaswamy, V., Seman, C. J., Shevliakova, E., Sirutis, J. J., Stern, W. F., Stouffer, R. J., Wilson, R. J., Winton, M., Wittenberg, A. T., and Zeng, F.: The Dynamical Core, Physical Parameterizations, and Basic Simulation Characteristics of the Atmospheric Component AM3 of the GFDL Global Coupled Model CM3, Journal of Climate, 24, 3484–3519, https://doi.org/10.1175/2011jcli3955.1, 2011.

Döscher, R., Acosta, M., Alessandri, A., Anthoni, P., Arsouze, T., Bergman, T., Bernardello, R., Boussetta, S., Caron, L.-P., Carver, G., Castrillo, M., Catalano, F., Cvijanovic, I., Davini, P., Dekker, E., Doblas-Reyes, F. J., Docquier, D., Echevarria, P., Fladrich, U., Fuentes-Franco, R., Gröger, M., v. Hardenberg, J., Hieronymus, J., Karami, M. P., Keskinen, J.-P., Koenigk, T., Makkonen, R., Massonnet, F., Ménégoz, M., Miller, P. A., Moreno-Chamarro, E., Nieradzik, L., van Noije, T., Nolan, P., O'Donnell, D., Ollinaho, P., van den Oord, G., Ortega, P., Prims, O. T., Ramos, A., Reerink, T., Rousset, C., Ruprich-Robert, Y., Le Sager, P., Schmith, T., Schrödner, R., Serva, F., Sicardi, V., Sloth Madsen, M., Smith, B., Tian, T., Tourigny, E., Uotila, P., Vancoppenolle, M., Wang, S., Wårlind, D., Willén, U., Wyser, K., Yang, S., Yepes-Arbós, X., and Zhang, Q.: The EC-Earth3 Earth system model for the Coupled Model Intercomparison Project 6, Geoscientific Model Development, 15, 2973–3020, https://doi.org/10.5194/gmd-15-2973-2022, 2022.

Dyrrdal, A. V., Skaugen, T., Stordal, F., and Førland, E. J.: Estimating extreme areal precipitation in Norway from a gridded dataset, Hydrological Sciences Journal, 61, 483–494, https://doi.org/10.1080/02626667.2014.947289, 2015.

Guilloteau, C., Chen, X., Leung, L. R., and Foufoula-Georgiou, E.: Amplified Mesoscale and Submesoscale Variability and Increased Concentration of Precipitation under Global Warming over Western North America, Journal of Climate, 38, 2525–2542, https://doi.org/10.1175/jcli-d-24-0343.1, 2025.

Jacob, D., Teichmann, C., Sobolowski, S., Katragkou, E., Anders, I., Belda, M., Benestad, R., Boberg, F., Buonomo, E., Cardoso, R. M., Casanueva, A., Christensen, O. B., Christensen, J. H., Coppola, E., De Cruz, L., Davin, E. L., Dobler, A., Domínguez, M., Fealy, R., Fernandez, J., Gaertner, M. A., García-Díez, M., Giorgi, F., Gobiet, A., Goergen, K., Gómez-Navarro, J. J., Alemán, J. J. G., Gutiérrez, C., Gutiérrez, J. M., Güttler, I., Haensler, A., Halenka, T., Jerez, S., Jiménez-Guerrero, P., Jones, R. G., Keuler, K., Kjellström, E., Knist, S., Kotlarski, S., Maraun, D., van Meijgaard, E., Mercogliano, P., Montávez, J. P., Navarra, A., Nikulin, G., de Noblet-Ducoudré, N., Panitz, H.-J., Pfeifer, S., Piazza, M., Pichelli, E., Pietikäinen, J.-P., Prein, A. F., Preuschmann, S., Rechid, D., Rockel, B., Romera, R., Sánchez, E., Sieck, K., Soares, P. M. M., Somot, S., Srnec, L., Sørland, S. L., Termonia, P., Truhetz, H., Vautard, R., Warrach-Sagi, K., and Wulfmeyer,

https://doi.org/10.5194/egusphere-2026-207
Preprint. Discussion started: 6 March 2026

V.: Regional climate downscaling over Europe: perspectives from the EURO-CORDEX community, Regional Environmental Change, 20, https://doi.org/10.1007/s10113-020-01606-9, 2020.

Kahraman, A., Kendon, E. J., Chan, S. C., and Fowler, H. J.: Quasi-Stationary Intense Rainstorms Spread Across Europe Under Climate Change, Geophysical Research Letters, 48, https://doi.org/10.1029/2020gl092361, 2021.

Koutsoyiannis, D., Kozonis, D., and Manetas, A.: A mathematical framework for studying rainfall intensity-duration-frequency relationships, Journal of Hydrology, 206, 118–135, https://doi.org/10.1016/s0022-1694(98)00097-3, 1998.

Lind, P., Belušić, D., Christensen, O. B., Dobler, A., Kjellström, E., Landgren, O., Lindstedt, D., Matte, D., Pedersen, R. A., Toivonen, E., and Wang, F.: Benefits and added value of convection-permitting climate modeling over Fenno-Scandinavia, Climate Dynamics, 55, 1893–1912, https://doi.org/10.1007/s00382-020-05359-3, 2020.

Lind, P., Belušić, D., Médus, E., Dobler, A., Pedersen, R. A., Wang, F., Matte, D., Kjellström, E., Landgren, O., Lindstedt, D., Christensen, O. B., and Christensen, J. H.: Climate change information over Fenno-Scandinavia produced with a convection-permitting climate model, Climate Dynamics, https://doi.org/10.1007/s00382-022-06589-3, 2022.

Lutz, J., Grinde, L., and Dyrrdal, A. V.: Estimating Rainfall Design Values for the City of Oslo, Norway—Comparison of Methods and Quantification of Uncertainty, Water, 12, 1735, https://doi.org/10.3390/w12061735, 2020.

Mandelbrot, B. B.: Fractals and Scaling in Finance: Discontinuity, Concentration, Risk. Selecta Volume E, Springer New York, https://doi.org/10.1007/978-1-4757-2763-0, 1997.

Médus, E., Thomassen, E. D., Belušić, D., Lind, P., Berg, P., Christensen, J. H., Christensen, O. B., Dobler, A., Kjellström, E., Olsson, J., and Yang, W.: Characteristics of precipitation extremes over the Nordic region: added value of convection-permitting modeling, Natural Hazards and Earth System Sciences, 22, 693–711, https://doi.org/10.5194/nhess-22-693-2022, 2022.

Nhat, L. M., Tachikawa, Y., Sayama, T., and Takara, K.: A simple scaling charateristics of rainfall in time and space to derive intensity duration frequency relationships, Proceedings of Hydraulic Engineering, 51, 73–78, https://doi.org/10.2208/prohe.51.73, 2007.

Oguz, E. A., Benestad, R. E., Parding, K. M., Depina, I., and Thakur, V.: Quantification of climate change impact on rainfall-induced shallow landslide susceptibility: a case study in central Norway, Georisk: Assessment and Management of Risk for Engineered Systems and Geohazards, 18, 467–490, https://doi.org/10.1080/17499518.2023.2283848, 2024.

Parding, K. M., Benestad, R. E., Dyrrdal, A. V., and Lutz, J.: A principal-component-based strategy for regionalisation of precipitation intensity–duration–frequency (IDF) statistics, Hydrology and Earth System Sciences, 27, 3719–3732, https://doi.org/10.5194/hess-27-3719-2023, 2023.

Rodríguez, R., Navarro, X., Casas, M. C., Ribalaygua, J., Russo, B., Pouget, L., and Redaño, A.: Influence of climate change on IDF curves for the metropolitan area of Barcelona (Spain), International Journal of Climatology, 34, 643–654, https://doi.org/10.1002/joc.3712, 2013.

Roksvåg, T., Lutz, J., Grinde, L., Dyrrdal, A. V., and Thorarinsdottir, T. L.: Consistent intensity-duration-frequency curves by post-processing of estimated Bayesian posterior quantiles, Journal of Hydrology, 603, 127 000, https://doi.org/10.1016/j.jhydrol.2021.127000, 2021.

Sorteberg, A, Lawrence, D, Dyrrdal, A V, Mayer, S, and Engeland, K: Climatic changes in short duration extreme precipitation and rapid onset flooding - implications for design values, NCCS report 1/2018, Norwegian Climate Change Services, Oslo, Norway, 2018.

Trenberth, K. E., Dai, A., Rasmussen, R. M., and Parsons, D. B.: The Changing Character of Precipitation, Bulletin of the American Meteorological Society, 84, 1205–1218, https://doi.org/10.1175/bams-84-9-1205, 2003.

Vinnarasi, R. and Dhanya, C.: Time-varying Intensity-Duration-Frequency relationship through climate-informed covariates, Journal of Hydrology, 604, 127 178, https://doi.org/10.1016/j.jhydrol.2021.127178, 2022.

https://doi.org/10.5194/egusphere-2026-207
Preprint. Discussion started: 6 March 2026

Yu, P.-S., Yang, T.-C., and Lin, C.-S.: Regional rainfall intensity formulas based on scaling property of rainfall, Journal of Hydrology, 295, 108–123, https://doi.org/10.1016/j.jhydrol.2004.03.003, 2004.